Accepted Preprint first posted on 6 May 2016 as Manuscript JOE-15-0528

Hyperprolactinemia induced by hCG leads to metabolic disturbances in female mice

Abbreviated title: hCG hypersecretion and metabolism

Laura D. Ratner[1], Guillermina Stevens[1,5], Maria Marta Bonaventura[1], Victoria A. Lux-Lantos[1], Matti Poutanen[2,3], Ricardo S. Calandra[1], Ilpo T. Huhtaniemi[2,4], Susana B. Rulli[1].

[1] Instituto de Biología y Medicina Experimental- Consejo Nacional de Investigaciones Científicas y Técnicas, Vuelta de Obligado 2490, C1428ADN, Buenos Aires, Argentina.

[2] Department of Physiology, Institute of Biomedicine, University of Turku, Kiinamyllynkatu 10, FIN-20520 Turku, Finland.

[3] Turku Center for Disease Modeling, University of Turku, Kiinamyllynkatu 10, FIN-20520 Turku, Finland.

[4] Department of Surgery and Cancer, Imperial College London, London W12 0NN, UK.

[5] Hospital General de Agudos J. M. Ramos Mejía, Urquiza 609, Buenos Aires, Argentina.

Address all correspondence and reprint request to:

Dr. Susana B. Rulli,

Instituto de Biología y Medicina Experimental,

Vuelta de Obligado 2490 C1428ADN, Buenos Aires, Argentina.

TEL: +54 11 47832869, ext. 212. FAX: +54 11 47862564.

E-mail:srulli@ibyme.conicet.gov.ar; rulli.susana@gmail.com

Word count: 4994

2. Abstract

The metabolic syndrome is a growing epidemic; it increases the risk for diabetes, cardiovascular disease, fatty liver and several cancers. Several reports have indicated a link between hormonal imbalances and insulin resistance or obesity. Transgenic (TG) female mice overexpressing the human chorionic gonadotropin β-subunit (hCGβ+ mice) exhibit constitutively elevated levels of hCG, increased production of testosterone, progesterone and prolactin, and obesity. The objective of this study was to investigate the influence of hCG hypersecretion on possible alterations in the glucose and lipid metabolism of adult TG females. We evaluated fasting serum insulin, glucose and triglyceride levels in adult hCGβ+ females and conducted intraperitoneal glucose and insulin tolerance tests at different ages. TG female mice showed hyperinsulinemia, hypertriglyceridemia and dyslipidemia, as well as glucose intolerance and insulin resistance at 6 months of age. A one-week treatment with the dopamine agonist cabergoline applied on 5-week-old hCGβ+ mice, which corrected hyperprolactinemia, hyperandrogenism, and hyperprogesteronemia, effectively prevented the metabolic alterations. These data indicate a key role of the hyperprolactinemia-induced gonadal dysfunction in the metabolic disturbances of hCGβ+ female mice. The findings prompt further studies on the involvement of gonadotropins and prolactin on metabolic disorders and might pave the way for the development of new therapeutic strategies.

Key words: human chorionic gonadotropin, insulin resistance, transgenic mice, prolactin

3. Introduction

Metabolic syndrome is a growing epidemic worldwide that involves 1 out of 4 adult people, and its prevalence increases with age (Grundy, 2008). The consensus statement provided by the International Diabetes Federation (IDF) defines the metabolic syndrome as a condition with abdominal obesity plus any two of the following: elevated plasma triglyceride levels, reduced high-density lipoproteins (HDL), increased blood pressure, or increased fasting plasma glucose (Alberti et al., 2006). Obesity-associated insulin resistance is considered a cause-and-effect relationship since weight changes correlate with changes in insulin sensitivity (Kahn et al., 2006, Qatanani and Lazar, 2007). In this respect, hyperlipidemia is linked to insulin resistance, since insulin promotes fat cell differentiation, enhances adipocyte glucose uptake, and inhibits adipocyte lipolysis.

Although the role of prolactin in reproduction is well known, the participation of this hormone in weight gain and glucose homeostasis is still under debate. Patients with prolactinomas were reported to acquire weight gain and metabolic alterations (Greenman et al., 1998; Ben-Jonathan et al., 2008). However, it is still unclear whether these conditions are directly associated to hyperprolactinemia (Ciresi et al., 2013). Recent experimental evidence suggests that prolactin has a crucial role on the pancreas and the adipose tissue, most notably during development. Prolactin receptor deficient mice (*Prlr-/-*) provided direct evidence that prolactin signaling is involved in adipogenesis by affecting energy balance and metabolic adaptation (Carre and Binart, 2014). Furthermore, prolactin is shown to be essential for the pancreatic β-cell development during the perinatal period (Auffret et al., 2013), and is therefore, involved in the manifestation of insulin resistance by stimulating insulin release and regulating adipokine release (Ben-Jonathan et al., 2008;

Carre and Binart, 2014). Prolactin was found to decrease glucose transporter 4 (GLUT 4) mRNA expression that may cause a decreased glucose uptake in peripheral tissues (Nilsson et al., 2009). Moreover, prolactin induces pyruvate dehydrogenase kinase 4 (PDK4), whose activation is known to lead to decreased glucose oxidation (White et al., 2007). In addition, this hormone participates in perinatal brown adipocyte differentiation and function (Viengchareum et al., 2008), and also affects energy homeostasis through modulation of lipid metabolism (Carre and Binart, 2014).

We have previously shown the implications of chronically elevated levels of hCG in the phenotype of transgenic (TG) mice. Particularly, female mice overexpressing the hCGβ- subunit (hCGβ+) exhibit precocious puberty, elevated serum levels of hCG, prolactin, testosterone and progesterone, and present with infertility (Rulli et al., 2002; Ratner et al., 2012). Besides, hCGβ+ ovaries show hemorrhagic cysts and massive luteinization as a result of the active stimulation with hCG (Rulli et al., 2002; Ratner et al., 2012). Among the extragonadal phenotypes, these females develop obesity, pituitary macroprolactinomas, mammary gland tumors and elevated bone density at older ages (Rulli et al., 2002; Yarram et al., 2003; Kuorelahti et al., 2007; Ahtiainen et al., 2010; Ratner et al., 2012). In contrast to transgenic females, hCGβ+ males are fertile and exhibit normal levels of testosterone and prolactin (Rulli et al., 2003).

Even though LH/hCG receptors are detected in different non-gonadal tissues, including the pancreas (Abdallah et al., 2004; Cole, 2010), their physiological significance remains unclear. Our previous studies demonstrate that hyperprolactinemia is the main cause for the reproductive defects of adult hCGβ+ females, which can be prevented by a short-term treatment with the dopamine agonist cabergoline at the beginning of the reproductive age (Ratner et al., 2012). Conversely, the same treatment applied at 3 months

of age failed to recover fertility. These findings demonstrate that the cabergoline treatment applied at a critical moment of the phenotype progression prevents hCG-induced abnormalities in these transgenic mice.

The aim of this study was to investigate the possible alterations of glucose and lipid metabolism in adult hCGβ+ females. The short-term treatment with cabergoline was followed in order to assess whether hyperprolactinemia influenced metabolism in the hypersecreting hCGβ females. Since hCGβ+ males do not exhibit changes in prolactin levels, this study was focused on females. Glucose and insulin tolerance tests were conducted at different ages, as well as determination of serum insulin concentration and pancreatic gene expression analysis. Since obesity was described as part of the extra-gonadal phenotype, serum triglycerides, cholesterol and high density lipoprotein cholesterol (HDL-C) were also measured in TG females.

4. Materials and Methods

Animals

All the experiments were performed in TG female mice overexpressing the hCGβ-subunit under the control of the human ubiquitin C promoter (hCGβ+). Generation, housing and genotyping of hCGβ+ with FVB/N genetic background have been previously described (Rulli et al., 2002). Wild-type (WT) littermates were used as controls. Mice were maintained under controlled conditions (12-h light/dark cycle, 21 C), and were given free access to laboratory chow and tap water. Food intake was monitored daily on females caged individually during one week. All experimental procedures were performed according to the NIH Guidelines for Care and Use of Experimental Animals, and approved

by the Institutional Animal Care and Use Committee of the Instituto de Biología y Medicina Experimental, Consejo Nacional de Investigaciones Científicas y Técnicas (IBYME-CONICET).

Cabergoline treatment

WT and hCGβ+ female mice of 5 weeks of age were injected ip with 500 μg/kg of cabergoline (Laboratorios Beta S.A., Buenos Aires, Argentina) suspended in 0.25% (w/v) methylcellulose as vehicle (Tanaka and Ogawa, 2005). The females received three injections of cabergoline, one every other day, during 1 week (hCGβ+cab) (Ratner et al., 2012). The females used as controls were injected with vehicle only.

Glucose homeostasis tests

Two, three and 6-month-old female mice were fasted for 6 or 3 hr and blood was collected from the tail vein, to perform glucose tolerance test (IGTT) or insulin tolerance test (ITT) respectively. Glucose (2 g/kg, dissolved in water) or insulin (0,75 IU/kg Humulin R, Eli Lilly Interamericana, Argentina) was administered by i.p. injection. Blood glucose was determined at time points 0, 30, 60 and 90 min according to manufacturer´s recommendations by using a glucometer Accu-Chek (Roche) (Andrikopoulos et al., 2008).The ITT was performed on the same group of animals one week after IGTT. In addition, glucose-stimulated insulin secretion was determined from serum samples of 6-hour-fasted females of 3 and 6 months of age, at 0 and 30 min after glucose administration. Serum samples were obtained by centrifugation and stored at -20 C. Insulin levels were assessed by rat/mouse insulin Elisa kit (EZRMI-13K; Millipore).

145 **Sample collection**

146 Mice were weighed and euthanized by CO_2 asphyxiation at 6 months of age after 18
147 hr fasting, and cardiac blood was obtained immediately thereafter. Serum samples were
148 separated by centrifugation and stored at -20 C for biochemical analyses. Pancreata were
149 perfused with RNAlater (Ambion) immediately after dissection, and then snap frozen and
150 stored at -70 C for RNA isolation.

151

152 **Biochemical analyses**

153 Serum cholesterol, triglycerides and high density lipoprotein cholesterol (HDL-C)
154 concentrations were measured by colorimetric assays (BioSystems, Spain) according to the
155 manufacturer's instructions. Serum lipid indices were calculated according to the following
156 formulas: Cholesterol / HDL-C (Castelli, 1996); Triglycerides / HDL-C (McLaughlin et al.,
157 2003). The calculation of HOMA-IR (Homeostasis Model Assessment Insulin Resistance)
158 was performed according to the formula of Matthews et al. (1985): (Glucose mmol / dl x
159 Insulin mUI / ml) / 22.5. The Quicki (Quantitative Insulin Sensitivity Check Index) was
160 calculated consistent with Katz et al. (2000): 1 / (Log Insulin mUI / ml + Log Glucose mg /
161 dl).

162

163 **hCG bioassay**

164 The bioactive levels of circulating hCG were determined by the mouse testicular
165 interstitial cell *in vitro* bioassay as previously described (Ding and Huhtaniemi, 1989; Rulli
166 et al, 2002). Briefly, decapsulated testes from adult WT males were dispersed with
167 collagenase type I (0.15 mg/ml) in M199 medium (Sigma-Adrich) for 5 min at 34 C. The
168 supernatant was filtered through nylon mesh (mesh size 100 μm) and the cell suspension

was washed twice with M199 medium supplemented with 0.1% (w/v) bovine serum albumin (BSA; Sigma-Aldrich) and 20mM HEPES (Sigma-Aldrich). Testicular interstitial cells obtained using this technique are predominantly Leydig cells, as described previously (Ding and Huhtaniemi, 1989). Cells (50 000 cells/tube) were incubated with increasing concentrations of recombinant hCG as standard (AFP8456A, 20000 IU/mg; NHPP, NIDDK), or with the serum samples, in a 95%O_2/5%CO_2 atmosphere at 34 C for 4 h. After incubation, supernatants were recovered by centrifugation and frozen at -20 C. The testosterone concentration in the supernatants was measured by radioimmunoassay, according to a method described previously (Ratner et al., 2012). The intra- and inter-assay coefficients of variation were less than 12%.

***In vivo* peripheral tissue response to insulin**

Six-month-old WT and hCGβ+ female mice were fasted for 4 h. Then, animals were anesthetized with 2% avertin (12 ml/kg i.p.). The abdominal cavity was opened and 2 IU/kg of insulin was injected into the portal vein. At time points 0 and 5 min post-injection, portions of skeletal muscle were excised and flash frozen in liquid N_2 and stored at −70 C until used.

Western blot analysis

Skeletal muscle homogenates were prepared with lysis buffer (50 mM TRIS, 150 mM $NaCl_2$, 1mM EDTA, 0.1%SDS, 0.5% sodium deoxycholate, 1% NP40-IGEPAL), 200 mM sodium orthovanadate (NO_3VO_4), 200mM NaF and protease inhibitor cocktail (Roche). Concentration was determined by the method of Lowry (1951), using BSA as standard protein. Fifteen μg of protein from each sample was resolved by 10% SDS-PAGE

193 under reducing conditions and transferred to nitrocellulose membranes (Amersham
194 Hybond-ECL, GE Healthcare Life Sciences, Pittsburgh, PA, USA). To reduce non-specific
195 antibody binding, membranes were incubated for 1 h at room temperature in T-TBS
196 blocking buffer. The membranes were then incubated overnight at 4 C with antibodies anti-
197 AKT and anti-pAKT in T-TBS, 1% BSA (Cell Signalling, MA; AKT, #9272S:1/500;
198 pAKT, #4060S: 1/2000). Secondary goat anti-rabbit antibody conjugated with peroxidase
199 HRP (Santa Cruz Biotechnology inc, CA, # sc-2004: 1/5000) were used. For actin
200 detection, membranes were incubated overnight at 4 C with first antibody diluted in PBS-T,
201 1% BSA (Calbiochem CA, # cp01: 1:5000) followed by incubation with secondary goat
202 anti-mouse IgM antibody conjugated with peroxidase HPR (Santa Cruz Biotechnology Inc,
203 CA, # sc-2064:1/2000). Immunoreactive proteins were revealed by enhanced
204 chemiluminescence (ECL-Plus, Amersham, GE Healthcare LifeSciences) using hyperfilm
205 ECL (GE Healthcare LifeSciences) and band intensities were quantified using Scion
206 Analyzer software.
207
208 **Immunohistochemistry**
209 Pancreata from 6-month-old WT, hCGβ+ and hCGβ+cab female mice were fixed in
210 4% paraformaldehyde, dehydrated and embedded in paraffin wax. Endogenous peroxidase
211 reactivity was quenched by a 20-min pretreatment with 10% methanol, 0.3% H_2O_2 in
212 0.01M PBS (pH 7.4). For antigenic retrieval, sections were pretreated with citrate buffer
213 (0.01M, pH 6), and permeabilized by a 5-min incubation with 0.5% saponin in PBS and 5-
214 min incubation with proteinase K (10 ng/ml). Non-specific proteins were blocked by
215 subsequent incubation with protein blocking buffer (5% goat normal serum in PBS for
216 Pdx1, and 5% horse normal serum in PBS for Nkx 6.1) for 30 min. After several wash

steps, sections were incubated with antibodies rabbit anti-Pdx1 (Millipore, CA, # 06-1379: 1/1000) and mouse anti-Nkx 6.1 (DSHB, # F55A10-S: 1/250) diluted in incubation buffer (2% goat normal serum in PBS for Pdx1; 2% horse normal serum in PBS for Nkx 6.1) overnight in a humidified chamber at 4 C. On the second day, pancreata sections were washed and incubated with biotinylated secondary antiserum (goat anti-rabbit IgG; horse anti-mouse IgG, 1:500, Vector Lab., CA, USA) for 2h at room temperature. Finally, immunoreaction was visualized with 0.01% H_2O_2 and 0.05% 3,3-diaminobenzidine solution (in 0.05 M Tris–HCl, pH 7.6) and an avidin–biotin–peroxidase system (Vector Lab). Negative controls were performed in the absence of the primary antibodies.

RNA isolation and analysis of gene expression

Total RNA was isolated from pancreata as previously described (Gonzalez et al., 2011), using TRIZOL reagent (Invitrogen) according to the manufacturer's protocol. Two micrograms of RNA were treated with DNAse I (Invitrogen) and reverse-transcribed in a 20 µl reaction volume using M-MLV reverse transcriptase (Promega) and random hexameres (Biodynamics). For quantitative real-time PCR (qPCR) primer sets were designed for the specific amplification of *Ins1, Ins2, Gcg* (*Ins1* Fw: AAGCTGGTGGGCATCCAGTAACC, *Ins1* Rev: GTTTGGGCTCCCAGAGGGCAAG; *Ins2* Fw: CCCTGCTGGCCCTGCTCTT, *Ins2* Rev: AGGTCTGAAGGTCACCTGCT; *Gcg* Fw: CTACACCTGTTCGCAGCTCA, *Gcg* Rev: CTGGGGTTCTCCTCTGTGTC), and cyclophilin A (*Ppia)* as an internal control (*Ppia* Fw: GCGTCTCCTTCGAGCTGTT, *Ppia* Rev: AAGTCACCACCCTGGCAC). Each sample was assayed in duplicate using 4 pmol of each primer, SYBR Green Master Mix (Applied Biosystems) and 2-20ng of cDNA in a total volume of 15 µl. Amplification was carried out in a CFX96 Touch™ Real-Time PCR

Detection System (Bio-Rad). For the assessment of quantitative differences in the cDNA target between samples the mathematical model of Pfaffl (2001) was applied. An expression ratio was determined for each sample by calculating $(E_{target})^{\Delta Ct\ (target)}/(E_{Ppia})^{\Delta Ct\ (Ppia)}$, where E is the efficiency of the primer set and ΔCt= Ct (reference cDNA) – Ct (experimental cDNA). The amplification efficiency of each primer set was calculated from the slope of a standard amplification curve of log (nanograms of cDNA) per reaction vs. Ct value ($E = 10^{-(1/slope)}$). Efficiencies of 2±0.1 were considered optimal. Results were expressed relative to a reference sample (WT choosen *ad random*).

Statistical Analysis

Data are expressed as the mean ± SEM. Statistical analysis for comparing two sets of data was performed with Student's t test for two independent groups. In those experiments where the effects of two factors (genotype and treatment) were studied, the two-way ANOVA was performed. The two-way ANOVA with repeated measures was used for the glucose and insulin tolerance tests. Bonferroni's post-hoc test was used to establish the level of significance between group pairs. The trapezoidal rule was used to determine the area under the curve (AUC). Data were transformed when required. A p value less than 0.05 was considered significant.

5. Results

Hormonal and metabolic status of hCGβ+ female mice

We have previously demonstrated that at 6 months of age, hCGβ+ female mice showed pronounced disturbances in their gonadal and non gonadal phenotype (Rulli et al., 2002; Ratner et al., 2012). As was confirmed in Table 1, hCGβ+ females exhibited a

265 significant increase in body weight, abdominal white fat depot and serum levels of
266 bioactive hCG as compared with WT ($p<0.01$) (Rulli et al., 2002; Ratner et al., 2012). This
267 change, however, was not accompanied by an increase in the daily food intake. At this age,
268 serum levels of insulin and triglycerides were elevated in TG females ($p<0.001$). On the
269 other hand, serum fasting glucose, cholesterol and HDL-C levels did not show differences
270 between WT and hCGβ+ females (Table 1). In addition, the atherogenic (or Castelli) index,
271 represented by the ratio of cholesterol/HDL-C, did not show significant differences
272 between the groups, whereas the triglycerides/HDL-C ratio showed a statistically
273 significant increase in hCGβ+ females as compared with WT females ($p < 0.001$). From
274 fasting insulin and glucose data, we calculated the surrogate indexes of insulin sensitivity
275 and resistance HOMA-IR and QUICKI. The values of HOMA-IR were significantly higher
276 in the hCGβ+ group compared with WT ($p<0.05$; Table 1), as observed for groups of mice
277 with decreased insulin sensitivity. Conversely, the value of QUICKI was significantly
278 lower in the hCGβ+ group compared with WT ($p<0.05$), also indicative of diminished
279 insulin sensitivity.
280
281 **Age-dependent changes in the glucose homeostasis of hCGβ+ females**
282 In order to study a possible correlation with age, IGTT and ITT were performed in
283 2, 3 and 6-month-old WT and hCGβ+ females. No differences were found in IGTT at two
284 months of age (Fig. 1 A). At 3 and 6 months of age, TG females showed glucose
285 intolerance, represented by a delay in glucose clearance and an increase in glucose levels
286 through the different time-points analyzed after glucose administration (Fig. 1 B,C).
287 Accordingly, the total glucose levels accumulated during the 90 min of the assay,

represented as the AUC, were significantly increased in hCGβ+ females as compared with WT ($p<0.01$).

The ITT performed in 2 and 3 month-old TG females showed a quick decline in glucose levels at 30 min after insulin administration, and remained low thereafter, as it was observed in WT females at the same ages (Fig. 2 A,B). However, 6-month-old hCGβ+ females showed elevated glucose levels after insulin administration, which remained high through the different time-points analyzed (Fig. 2 C). Accordingly, the AUC resulted elevated in hCGβ+ females ($p<0.01$).

The insulin secretion capacity in response to glucose administration was performed in 3- and 6-month-old WT and hCGβ+ females (Fig. 3A). The glucose response was first measured at 30 min, meaning that only the second phase of insulin secretion was detected in this study (Caumo and Luzi, 2004). TG mice from both ages exhibited elevated basal insulin levels as compared with WT females. The insulin secretion of WT females from both ages showed a correct response to glucose stimulation with at least a 2.5- fold increase at 30 min post-glucose administration ($p<0.05$). Conversely, 3- and 6-month-old hCGβ+ mice exhibited an impaired glucose- stimulated response, being only a 0.8 and 1- fold increase, respectively (Fig. 3A).

Since TG female mice showed profound alterations in glucose metabolism at 6 months of age, we further analyzed the peripheral insulin sensitivity at this age. To this aim, we determined the status of insulin- induced AKT phosphorylation in skeletal muscle obtained from fasted WT and hCGβ+ mice (Fig 3B). As expected, WT females showed a 3-fold increase in insulin-stimulated AKT phosphorylation ($p<0.05$), whereas TG females exhibited a severely impaired AKT activation, with levels comparable to basal of both

311 groups ($p<0.05$). TG females showed an increase in total AKT as compared with WT
312 ($p<0.05$).

313 Taken together these results showed that 6-month-old hCGβ+ females exhibited
314 peripheral insulin resistance and impaired glucose tolerance, being the most important
315 disruptions in glucose homeostasis.

316

317 **Effect of cabergoline on the glucose and lipid homeostasis of hCGβ+ females.**

318 Treatment with the dopaminergic agonist cabergoline was carried out to analyze the
319 influence of hyperprolactinemia on serum insulin, glucose and triglycerides. It was
320 confirmed that a short-term treatment with cabergoline administered at 5 weeks of age to
321 hCGβ+ females (hCGβ+cab) was effective in the normalization of prolactin levels
322 ($p<0.001$; Fig 4B) and body weight ($p<0.05$; Fig 4 A) at 6 months of age (Ratner et al.,
323 2012). In addition, cabergoline treatment restored serum triglycerides ($p<0.001$; Fig. 4 D)
324 and insulin ($p<0.05$; Fig. 4 C) to normal levels in comparison to hCGβ+ control females.
325 Cabergoline treatment administered to 5-week-old WT females (WTcab), did not produce
326 any effect on the parameters studied (Fig. 4 A-D).

327

328 **Effect of cabergoline on IGTT and ITT of hCGβ+ females**

329 IGTT and ITT were performed to further analyze the influence of prolactin on the
330 glucose homeostasis of the TG females (Fig. 5). The IGTT showed a similar clearance in
331 WT and WTcab females, with significantly increased glucose levels of hCGβ+ females at
332 30, 60 ($p<0.001$) and 90 ($p<0.01$) min after glucose administration (Fig. 5 A). hCGβ+
333 females treated with cabergoline showed a significant reduction of the glucose levels at 30

min, as compared with the results obtained for hCGβ+ females. In line with this, the AUC exhibited similar results (Fig. 5 B).

The ITT demonstrated that cabergoline treatment fully prevented the appearance of insulin resistance in TG females (Fig. 5 C). This was confirmed by analyzing the AUC: complete normalization occurred in cabergoline treated TG females with respect to control hCGβ+ females ($p<0.05$; Fig. 5 D).

Effect of cabergoline on pancreatic *Ins1, Ins2*, *Gcg, Pdx1 and Nkx 6.1* in hCGβ+ females.

Due to the effectiveness of the cabergoline treatment in normalizing the glucose homeostasis of TG females, we assessed gene expression for preproinsulin (*Ins1* and *Ins2*) and glucagon (*Gcg*) in pancreatic tissue of 6-month-old hCGβ+ and hCGβ+cab females. In agreement with the increased serum levels of insulin, hCGβ+ females exhibited significantly increased gene expression of both *Ins1* and *Ins2,* as compared with WT females ($p<0.05$, Fig 6A). The cabergoline treatment restored the expression levels of the genes for insulin to the level obtained in WT mice (Fig. 6 A). In contrast, the expression of *Gcg* did not show significant differences among the groups studied (Fig. 6A). The cabergoline treatment applied to WT females did not affect the expression levels of the genes analyzed.

In addition, we performed immunohistochemistry for two well known markers of β-cell maturity and identity, PDX1 and NKX 6.1. The presence of both markers was detected in the pancreatic islets of WT, hCGβ+ and hCGβ+cab, and the expected nuclear localization was observed (Fig 6B).

6. Discussion

The influence of hormones on glucose and lipid metabolism may be evidenced, among others, in various clinical conditions such as hormone replacement therapy, pregnancy, menopause, and hyperandrogenic states. Several models have been useful for understanding the pathophysiology of the metabolic syndrome (Kennedy et al., 2010; Guo, 2014). We report here a TG mouse model that shows a clear link between alterations of the gonadotropin axis and metabolic dysfunctions.

As previously demonstrated, hCGβ+ females exhibit elevated levels of hCG, progesterone, testosterone and prolactin, precocious puberty associated with a transient increase of serum estradiol, and infertility at adulthood (Rulli et al., 2002; Ratner et al., 2012). Besides, hCGβ+ females show obesity, mainly with abdominal fat accumulation, macroprolactinomas, mammary adenocarcinoma and increased bone mineral density at older ages (Rulli et al., 2002; Yarram et al., 2003; Ahtiainen et al., 2010; Kuorelahti et al., 2010; Bachelot et al., 2013). These extra-gonadal phenotypes of the hCGβ+ females are abolished by gonadectomy, indicating that ovarian hCG hyperstimulation with abnormal gonadal hormone production is directly or indirectly responsible for the extra-gonadal phenotype observed in this model (Rulli et al., 2002). Furthermore, we have shown that a short-term treatment with the dopamine agonist cabergoline to hCGβ+ females abolishes hyperprolactinemia, normalizes steroid hormone levels, and prevents the development of mammary tumors and pituitary adenomas in adulthood, thus, demonstrating the pivotal role of prolactin on certain phenotypic alterations of hCGβ+ females (Ratner et al., 2012). In the present study, we showed that the endocrinological alterations induced by chronic hCG overproduction lead to significant metabolic dysfunctions associated with hyperinsulinemia, glucose intolerance and impaired glucose- stimulated insulin secretion

382 that precedes/accompanies the development of insulin resistance. The failure of β-cell
383 function in this model is evident, since despite hyperinsulinemia, basal glucose ranged
384 within the normal values, but not after an i.p. glucose load. Besides, hypertriglyceridemia
385 and high triglyceride/HDL-C index were found in adult female mice.

386 It is well known that AKT activation is involved in insulin sensitivity in peripheral
387 organs. Specifically, in the skeletal muscle insulin activates, via IRS-1, the signalling
388 pathways that involve phosphatidylinositol (PI) 3-kinase and its downstream effector AKT,
389 which mediates glucose uptake by leading to membrane translocation of GLUT 4
390 (Bjornholm et al., 1997). Given the evidence of insulin resistance and hyperinsulinemia
391 with normoglycemia in TG females, we analyzed the activation of akt in skeletal muscle. It
392 seems that two phenomena coexist in this model. Firstly, high basal AKT expression with
393 the consequent increase in basal AKT phosphorylation, and secondly the impaired AKT
394 activation after insulin stimulation. A similar situation was found in a mouse model under
395 high fat diet (Liu et al., 2009). These animals also showed insulin resistance and
396 hyperinsulinemia with normoglycemia. Moreover, basal AKT phosphorylation was
397 increased, thus showing an adaptation of the system to the high insulin levels, and allowing
398 the maintenance of glucose levels within the normal range (Liu et al., 2009). In the same
399 way, we found an increase in basal AKT phosphorylation that would explain the
400 normoglycemia observed. These findings, together with the inability to respond to
401 exogenous insulin stimulation, suggest that the high AKT protein levels would lead to a
402 saturation of the AKT kinase activity, thus producing a decrease in the rate of insulin-
403 stimulated phosphorylation and explaining the insulin resistance observed in our model.
404 Similar results were observed in humans, with altered AKT activation in skeletal muscle
405 under hyperinsulinemic conditions (Karlsson et al., 2005). In addition, the db/db mice

406 model, as well as obese diabetic human patients, also exhibit decreased AKT
407 phosphorylation but unaltered basal total AKT in skeletal muscle (Shao et al., 2000;
408 Gosmarov et al., 2004).

409 The role of prolactin on reproduction has been extensively studied, but implications
410 of this hormone on metabolism, body weight and energy regulations are an open issue.
411 Pregnant and lactating women exhibit hypoadiponectinemia due to prolactin influence on
412 secretion and expression of adiponectin (Asai-Sato et al., 2006). In hamsters, inhibition of
413 prolactin secretion by bromocriptine has led to a reduction in fat depots, without reducing
414 food intake or body weight (Freeman et al., 2000). It has been reported that prolactin is
415 involved in adipose tissue differentiation as well as regulation of energy expenditure
416 (Auffret et al., 2012). The absence of prolactin receptor in *Prlr* KO mice prevents high-fat
417 diet-induced weight gain, despite increased food intake through an increase in energy
418 expenditure and metabolic rate. In an opposite way, in our model, hyperprolactinemia
419 would be one of the main effectors on the weight gain by inducing accumulation of white
420 abdominal fat depot and decreasing energy expenditure, with no change in food intake.

421 The lactogenic hormones during pregnancy enhance insulin production in response
422 to the growing metabolic demands on the mother and affect pancreatic islet development in
423 the fetus (Ben-Jonathan et al., 2008). Interestingly, the hyperprolactinemic state due to a
424 selective disruption of the dopamine D2 receptor in the lactotropes of female mice
425 (lacDrd2KO) leads to increased body weight, triglycerides, and glucose intolerance, but the
426 response to insulin was preserved (Perez Millan et al., 2014). The short-term treatment with
427 cabergoline provoked a recovery of glucose tolerance and a complete reversal of the insulin
428 resistance, as well as a significant reduction in insulin and triglyceride levels. In this regard,
429 cabergoline effectively prevented the hyperprolactinemia-associated metabolic

dysfunctions in TG mice. These findings provide strong evidence that elevated prolactin has a key role for the metabolic alterations in hCG overproducing females by acting directly on the target organs, and indirectly via alteration of the steroid hormone production. This could be explained by the persistent stimulus of prolactin together with hCG. This induces a significant increase of ovarian *Lhcgr* accompanied by a massive ovarian luteinization, which results in elevated levels of progesterone and testosterone (Ratner et al., 2012).

Androgens affect lipid metabolism by increasing the activity of lipoprotein lipase and hepatic lipase, by causing an increase in triglycerides, LDL-C and decrease the levels of HDL-C (LaRosa, 1995). Estrogens, on the contrary, increase HDL-C and decrease LDL-C levels (Gillmer, 1992; Tikkanen, 1996). The influence of androgens on lipid metabolism was also demonstrated in female rats under prenatal androgen treatment, which developed dyslipidemia and hepatic steatosis in adulthood. These changes would be the consequence of increased adipose tissue and insulin resistance induced by prenatal androgenization (Demissie et al., 2008). A similar metabolic alteration has been described in adult rats following early postnatal administration of testosterone (Alexanderson et al., 2007). Exposure to high levels of gonadal steroids, especially testosterone and progesterone throughout life (Rulli et al., 2002), could be one of the predisposing factors for dyslipidemia in this TG model, which is reinforced by the presence of obesity and insulin resistance.

The characteristic hyperprolactinemia in hCGβ+ females is a possible player in the adaptation of the pancreas to an increased insulin demand. Some lines of evidence serve as support for this purpose, as activation of prolactin receptor in the pancreas may be responsible for the increase in islet β-cells during pregnancy (Ben-Jonathan, 2008; Huang

et al., 2009; Huang, 2013). *In vitro* exposure of islets to prolactin increases insulin secretion, β-cell proliferation and decreases the threshold of insulin response to glucose (Huang et al., 2009). On the other hand *Prlr* KO mice showed islet and β-cell hypoplasia, reduced pancreatic insulin mRNA levels, a blunted insulin secretory response to glucose, and mild glucose intolerance (Freemark et al., 2001). During pregnancy of heterozygous Prlr +/- mice, pancreatic islet adaptation to blood glucose and the functioning mass of β–cell is affected (Huang et al., 2009).

Sex hormones collectively have the ability to reduce the sensitivity to insulin. It is known that estrogen and progesterone increase the pancreatic secretion of insulin and induce insulin resistance (Garcia et al., 1983; Gonzalez et al., 2000; Livingstone and Collison, 2002). These behave as counterregulatory hormones of glucose homeostasis during the early stages of pregnancy, and as a result, β-cell hyperplasia and increased pancreatic insulin secretion is observed (Macotela et al., 2009).

Rats and mice have two structurally similar insulin genes, *Ins1* and *Ins2*. Both genes are functional but there is no consensus about their relative expression in rodent β-cells (Roderigo-Milne et al., 2002). Changes in glucose metabolism of hCGβ+ females were accompanied by a significant increase in the expression of both genes. This confirmed that hyperinsulinemia resulted from the overproduction of insulin in pancreatic β-cells of the hCGβ+ females. The identity of insulin- producing pancreatic β cells was confirmed by the visualization of the specific markers PDX1 and NKX 6.1 in hCGβ+ mice. Besides, cabergoline treatment was able to significantly reduce the *Ins1* and *Ins2* mRNA levels, in concordance with the normalization of serum insulin in transgenic females.

In light of Metabolic Syndrome as a growing epidemic, animal models are good tools to determine the pathophysiological basis of this disease and how increases the risk for other diseases. This transgenic model overexpressing hCG gives us the possibility to study the consequences of hormone alterations in metabolic dysfunctions. Hyperprolactinemia associated with an altered gonadal function would explain the altered lipid and glucose metabolism in hCGβ+ female mice, considering that all these changes were manifested after the occurrence of high levels of gonadal steroids and prolactin, which started at early age and persisted high throughout life. On the other hand, the presence and activation of LH/hCG receptors in pancreatic β cells suggests a role for LH/hCG as a potential regulator of insulin release (Parkash et al., 2015). Consequently, the potential direct participation of hCG in the metabolic process deserves future studies.

7. Declaration of interests

There is no conflict of interest that could be perceived as prejudicing the impartiality of the research reported.

8. Funding

This work was supported by grants from the National Agency of Scientific and Technological Promotion (PICT2006 Nº272 for S.B.R.; PICT2011 Nº414 for R.S.C.); CONICET (PIP 183 for S.B.R.); Roemmers Foundation, Argentina; Fundación René Barón, Argentina.

9. Acknowledgements

Cabergoline was a gift from Laboratorios Beta S.A., Argentina.

10. References

Abdallah MA, Lei ZM, Li X, Greenwold N, Nakajima ST, Jauniaux E, Rao CV 2004 Human fetal nongonadal tissues contain human chorionic gonadotropin/luteinizing hormone receptors. *J Clin Endocrinol Metab* 89 952-956.

Ahtiainen P, Sharp V, Rulli S, Rivero-Müller A, Mamaeva V, Röytta M, Huhtaniemi I 2010 Enhanced LH action in transgenic female mice expressing hCGβ-subunit induces pituitary prolactinomas; the role of high progesterone levels. *Endocr Relat Cancer* 17 611-621.

Alberti G, Zimmet P, Shaw J, Grundy SM 2006 The International Diabetes Federation consensus worldwide definition of the metabolic syndrome. Extracted from http://www.idf.org/webdata/docs/IDF Meta_def_final.pdf.

Alexanderson C, Eriksson E, Stener-Victorin E, Lystig T, Gabrielsson B, Lönn M, Holmäng A 2007 Postnatal testosterone exposure results in insulin resistance, enlarged mesenteric adipocytes, and an atherogenic lipid profile in adult female rats: comparisons with estradiol and dihydrotestosterone. *Endocrinology* 148 5369–5376.

Andrikopoulos S, Blair AR, Deluca N, Fam BC, Proietto J 2008 Evaluating the glucose tolerance test in mice. *Am J Physiol Endocrinol Metab* 295 1323–1332.

519 Asai-Sato M, Okamoto M, Endo M, Yoshida H, Murase M, Ikeda M, Sakakibara H,
520 Takahashi T, Hirahara F 2006. Hypoadiponectinemia in lean lactating women: prolactin
521 inhibits adiponectin secretion from human adipocytes. *Endocr J* 53 555-562.

522 Auffret J, Freemark M, Carré N, Mathieu Y, Tourrel-Cuzin C, Lombès M, Movassat J,
523 Binart N 2013 Defective prolactin signaling impairs pancreatic β-cell development during
524 the perinatal period. *Am J Physiol Endocrinol Metab* 305 E1309-E1318.

525 Auffret J1, Viengchareun S, Carré N, Denis RG, Magnan C, Marie PY, Muscat A, Fève B,
526 Lombès M, Binart N 2012 Beige differentiation of adipose depots in mice lacking prolactin
527 receptor protects against high-fat-diet-induced obesity. *FASEB J* 26 3728-3737.

528 Bachelot A, Carré N, Mialon O, Matelot M, Servel N, Monget P, Ahtiainen P, Huhtaniemi
529 I, Binart N 2013 The permissive role of prolactin as a regulator of luteinizing hormone
530 action in the female mouse ovary and extragonadal tumorigenesis. *Am J Physiol Endocrinol*
531 *Metab* 305 E845-E852.

532 Ben-Jonathan N, LaPensee CR, LaPensee EW 2008 What can we learn from rodents about
533 prolactin in humans? *Endocr Rev* 29 1–41.

534 Bjornholm M, Kawano Y, Lehtihet M, Zierath JR 1997 Insulin receptor substrate-1
535 phosphorylation and phosphatidylinositol 3-kinase activity inskeletal muscle from NIDDM
536 subjects after in vivo insulin stimulation. *Diabetes* 46 524 –527.

537 Carré N, Binart N 2014 Prolactin and adipose tissue. *Biochimie* 97 16-21.

538 Castelli WP 1996 Lipids, risk factors and ischaemic heart disease. *Atherosclerosis* 124 S1-
539 S9.

Caumo A, Luzi L 2004 First-phase insulin secretion: does it exist in real life? Considerations on shape and function. *Am J Physiol Endocrinol Metab* 287 E371-E385.

Ciresi A, Amato MC, Guarnotta V, Lo Castro F, Giordano C 2013 Higher doses of cabergoline further improve metabolic parameters in patients with prolactinoma regardless of the degree of reduction in prolactin levels. *Clin Endocrinol (Oxf)* 79 845-852.

Cole LA 2010 Biological functions of hCG and hCG-related molecules. *Reprod Biol Endocrinol* 8 102–115.

Demissie M, Lazic M, Foecking EM, Aird F, Dunaif A, Levine JE 2008 Transient prenatal androgen exposure produces metabolic syndrome in adult female rats. *Am J Physiol Endocrinol Metab* 295 E262–E268.

Ding YQ, Huhtaniemi I 1989 Human serum LH inhibitor(s): behaviour and contribution to in vitro bioassay of LH using dispersed mouse Leydig cells. *Acta Endocrinol (Copenh)* 121 46-54.

Freeman ME, Kanyicska B, Lerant A and Nagy G 2000 Prolactin: structure, function, and regulation of secretion. *Physiol Rev* 80 1523-1631.

Freemark M, Fleenor D, Driscoll P, Binart N, Kelly P 2001 Body weight and fat deposition in prolactin receptor-deficient mice. *Endocrinology* 142 532–537.

García ME, Borelli MI, Gómez Dumm CL, Gagliardino JJ 1983 Functional and ultrastructural changes induced by short term ovariectomy on pancreatic islets. *Horm Metab Res* 15 76-81.

560 Gillmer MD 1992 Mechanism of action/effects of androgens on lipid metabolism. *Int J*
561 *Fertil* 37 83-92.

562 Gonzalez B, Ratner LD, Di Giorgio NP, Poutanen M, Huhtaniemi I, Calandra RS, Lux
563 Lantos VAR y Rulli SB 2011 Effect of chronically elevated androgens on the
564 developmental programming of the hypothalamic-pituitary axis in male mice. *Mol Cell*
565 *Endocrinol* 332 78-87.

566 González C, Alonso A, Alvarez N, Díaz F, Martínez M, Fernández S, Patterson AM 2000
567 Role of 17 β-estradiol and/or progesterone on insulin sensitivity in the rat: implications
568 during pregnancy. *J Endocrinol* 166 283–291.

569 Gosmanov AR, Umpierrez GE, Karabell AH, Cuervo R, Thomason DB 2004 Impaired
570 expression and insulin-stimulated phosphorylation of Akt-2 in muscle of obese patients
571 with atypical diabetes. *Am J Physiol Endocrinol Metab* 287 E8-E15.

572 Greenman Y, Tordjman K, Stern N 1998 Increased body weight associated with prolactin
573 secreting pituitary adenomas: weight loss with normalization of prolactin levels. Clin
574 *Endocrinol (Oxf)* 48547-553.

575 Grundy SM 2008 Metabolic syndrome pandemic. *Arterioscler Thromb Vasc Biol* 28 629-
576 636.

577 Guo S 2014 Insulin signaling, resistance, and metabolic syndrome: insights from mouse
578 models into disease mechanisms. *J Endocrinol* 220 T1–T23.

579 Huang C 2013 Wild-type offspring of heterozygous prolactin receptor-null female mice
580 have maladaptive β-cell responses during pregnancy. *J Physiol* 591 1325-1338.

581 Huang C, Snider F, Cross JC 2009 Prolactin receptor is required for normal glucose
582 homeostasis and modulation of β-cell mass during pregnancy. *Endocrinology* 150 1618–
583 1626.

584 Kahn SE, Hull RL, Utzschneider KM 2006 Mechanisms linking obesity to insulin
585 resistance and type 2 diabetes. *Nature* 444 840–846.

586 Karlsson HK, Zierath JR, Kane S, Krook A, Lienhard GE, Wallberg-Henriksson H 2005
587 Insulin-stimulated phosphorylation of the Akt substrate AS160 is impaired in skeletal
588 muscle of type 2 diabetic subjects. *Diabetes* 54 1692-1697.

589 Katz A, Nambi SS, Mather K, Baron AD, Follmann DA, Sullivan G, Quon MJ 2000
590 Quantitative insulin sensitivity check index: a simple, accurate method for assessing insulin
591 sensitivity in humans. *J Clin Endocrinol Metab* 85 2402-2410.

592 Kennedy AJ, Ellacott KL, King VL, Hasty AH 2010 Mouse models of the metabolic
593 syndrome. *Dis Model Mech* 3 156-166.

594 Kuorelahti A, Rulli S, Huhtaniemi I, Poutanen M 2007 Human chorionic gonadotropin
595 (hCG) up-regulates wnt5b and wnt7b in the mammary gland, and hCGbeta transgenic
596 female mice present with mammary gland tumors exhibiting characteristics of the
597 Wnt/beta-catenin pathway activation. *Endocrinology* 148 3694-3703.

598 LaRosa JC 1995 Androgens and women's health: Genetic and epidemiologic aspects of
599 lipid metabolism. *Am J Med* 98 S22-S26.

600 Liu HY, Hong T, Wen GB, Han J, Zuo D, Liu Z, Cao W 2009 Increased basal level of Akt-
601 dependent insulin signaling may be responsible for the development of insulin resistance.
602 *Am J Physiol Endocrinol Metab* 297 E898-906.

603 Livingstone C, Collison M 2002 Sex steroids and insulin resistance. *Clin Sci (Lond)* 102
604 151-166.

605 Lowry OH, Rosebrough NJ, Farr AL, Randall RJ 1951 Protein measurement with the Folin
606 phenol reagent. *J Biol Chem* 193 265-275.

607 Macotela Y, Boucher J, Tran TT, Kahn CR 2009 Sex and depot differences in adipocyte
608 insulin sensitivity and glucose metabolism. *Diabetes* 58 803-812.

609 Matthews DR, Hosker JP, Rudenski AS, Naylor BA, Treacher DF, Turner RC 1985
610 Homeostasis model assessment: insulin resistance and beta-cell function from fasting
611 plasma glucose and insulin concentrations in man. *Diabetologia* 28 412-419.

612 McLaughlin T, Abbasi F, Cheal K, Chu J, Lamendola C, Reaven G 2003 Use of metabolic
613 markers to identify overweight individuals who are insulin resistant. *Ann Intern Med* 139
614 802-809.

615 Nilsson LA, Roepstorff C, Kiens B, Billig H, Ling C 2009 Prolactin suppresses malonyl-
616 CoA concentration in human adipose tissue. *Horm Metab Res* 41 747-751.

617 Parkash J, Lei Z, Rao CV 2015 The Presence of Human Chorionic
618 Gonadotropin/Luteinizing Hormone Receptors in Pancreatic β-Cells. *Reprod Sci* 22 1000-
619 1007.

620 Pakarainen T, Ahtiainen P, Zhang FP, Rulli S, Poutanen M, Huhtaniemi I 2007
621 Extragonadal LH/hCG action--not yet time to rewrite textbooks. *Mol Cell Endocrinol* 269
622 9-16.

623 Perez Millan MI, Luque GM, Ramirez MC, Noain D, Ornstein AM, Rubinstein M, Becu-
624 Villalobos D 2014 Selective disruption of dopamine D2 receptors in pituitary lactotropes
625 increases body weight and adiposity in female mice. *Endocrinology* 155 829–839.

626 Pfaffl MW 2001 A new mathematical model for relative quantification in real-time RT-
627 PCR. *Nucleic Acids Res* 29 67-77.

628 Qatanani M, Lazar MA 2007 Mechanisms of obesity-associated insulin resistance: many
629 choices on the menu. *Genes Dev* 21 1443-1455.

630 Ratner LD, Gonzalez B, Ahtiainen P, Di Giorgio NP, Calandra RS, Huhtaniemi IT, Rulli
631 SB 2012 Short-term pharmacological suppression of the hyperprolactinemia of infertile
632 hCG-overproducing female mice persistently restores their fertility. *Endocrinology* 153
633 5980-5992.

634 Roderigo-Milne H, Hauge-Evans AC, Persaud SJ, Jones PM 2002 Differential expression
635 of insulin genes 1 and 2 in MIN6 cells and pseudoislets. *Biochem Biophys Res Commun*
636 296 589-595.

637 Rulli SB, Ahtiainen P, Mäkelä S, Toppari J, Poutanen M, Huhtaniemi I 2003 Elevated
638 steroidogenesis, defective reproductive organs, and infertility in transgenic male mice
639 overexpressing human chorionic gonadotropin. *Endocrinology* 144 4980-4990.

640 Rulli SB, Kuorelahti A, Karaer O, Pelliniemi LJ, Poutanen M, Huhtaniemi I 2002
641 Reproductive disturbances, pituitary lactotrope adenomas, and mammary gland tumors in
642 transgenic female mice producing high levels of human chorionic gonadotropin.
643 *Endocrinology* 143 4084-4095.

644 Shao J, Yamashita H, Qiao L, Friedman JE 2000 Decreased Akt kinase activity and insulin
645 resistance in C57BL/KsJ-Leprdb/db mice. *J Endocrinol* 167107-167115.

646 Tanaka KI, Ogawa N 2005 Dopamine agonist cabergoline inhibits levodopa-induced
647 caspase activation in 6-OHDA-lesioned mice. *Neurosci Res* 51 9-13.

648 Tikkanen MJ 1996 Estrogens, progestins and lipid metabolism from the International
649 Menopause Symposium. *Maturitas* 23 S51-S55.

650 Viengchareun S, Servel N, Fève B, Freemark M, Lombès M, Binart N 2008 Prolactin
651 receptor signaling is essential for perinatal brown adipocyte function: a role for insulin-like
652 growth factor-2. *PLoS One* 3 e1535.

653 White UA, Coulter AA, Miles TK, Stephens JM 2007 The STAT5A-mediated induction of
654 pyruvate dehydrogenase kinase 4 expression by prolactin or growth hormone in adipocytes.
655 *Diabetes* 56 1623-1629.

656 Yarram SJ, Perry MJ, Christopher TJ, Westby K, Brown NL, Lamminen T, Rulli SB,
657 Zhang FP, Huhtaniemi I, Sandy JR, Mansell JP 2003 Luteinizing Hormone Receptor
658 Knockout (LuRKO) Mice and Transgenic Human Chorionic Gonadotropin (hCG) -
659 Overexpressing Mice (hCGαβ+) Have Bone Phenotypes. *Endocrinology* 144 3555–3564.

660

11. Figure legends

Figure 1. Intraperitoneal Glucose Tolerance Test (IGTT) in hCGβ+ female mice at 2, 3 and 6 month of age. IGTT (2 g/kg) in fasted WT and hCGβ+ females was performed at 2 (A), 3 (B) (n=4), and 6 (C) months of age (n=7). Two-way ANOVA with repeated-measures, followed by Bonferroni's post hoc test was conducted; * $p<0.05$; ** $p<0.01$; *** $p<0.001$. The area under the curve (AUC) was analyzed for each group at different ages; Student´s t-test was conducted; ** $p<0.01$. Data are presented as mean±SEM.

Figure 2. Intraperitoneal Insulin Tolerance Test (ITT) in hCGβ+ female mice at 2, 3 and 6 month of age. ITT (0.75 IU/kg) in fasted WT and hCGβ+ females was performed at 2 (A), 3 (B) (n=4) and 6 (C) months of age (n=6). Two-way ANOVA with repeated-measures, followed by Bonferroni's post hoc test was conducted; * $p<0.05$; *** $p<0.001$. The area under the curve (AUC) was analyzed for each group at different ages; Student´s t-test was conducted; ** p<0-01. Data are presented as mean±SEM.

Figure 3. (A) Glucose- stimulated insulin release in 3- and 6-month-old hCGβ+ female mice. Glucose (2 g/kg) was administered i.p. to fasted WT and hCGβ+ female mice, and serum insulin levels were measured at 0 and 30 min post-glucose. Two-way ANOVA with repeated-measures, followed by Bonferroni's post hoc test was conducted. Data are presented as mean±SEM (n=4). *: $P<0.05$; **: $p<0.01$. (B) Peripheral tissue response to insulin. A representative western blot was shown for AKT activation in skeletal muscle. Samples were obtained from fasted 6-month-old WT and hCGβ+ female mice at 0 or 5 min after insulin administration. Two-way ANOVA followed by Bonferroni's post hoc test or

Student's t-test was conducted according to each case. Different letters indicate a value of at least $p<0.05$. Data are presented as mean±SEM (n=4).

Figure 4. Effect of cabergoline on body weight and serum levels of prolactin, insulin, and triglycerides in hCGβ+ females. Body weight (A) and serum prolactin (B), insulin (C) and trygicerides (D) levels in 6-month-old cabergoline- treated transgenic females (hCGβ+cab) (n=8) after 18 hr fasting. WT (n=12), cabergoline-treated WT (WTcab) (n=4) and hCGβ+ (n=8) females were used as controls. ANOVA, followed by Bonferroni's post hoc test was conducted. Different letters indicate a value of at least $p<0.05$. Data are presented as mean±SEM.

Figure 5. Effect of cabergoline treatment on the glucose homeostasis in WT and hCGβ+ females. IGTT (2 g/kg) (A), and ITT (0.75 IU/kg) (C) in fasted 6-month-old cabergoline-treated transgenic (hCGβ+cab) females was performed (n=8); fasted 6-month-old WT (n=12), cabergoline-treated WT (WTcab) (n=4) and hCGβ+ females (n=12) were used as control groups. Two-way ANOVA with repeated-measures, followed by Bonferroni's post hoc test was conducted. A) WT vs hCGβ+ **: $p<0.01$; ***: $p<0.001$; hCGβ+ vs hCGβ+cab ##: $p<0.01$; C) hCGβ+ vs WT, WTcab, hCGβ+cab; **: $p<0.01$, ***: $p<0.001$. The area under the curve (AUC) was analyzed for the different groups (B, D). ANOVA followed by Bonferroni's post hoc test was conducted. Different letters indicate a value of at least $p<0.05$. Data are presented as mean±SEM.

Figure 6. (A) Effect of cabergoline on the pancreatic gene expression of *Ins1, Ins2*, *Gcg* and *Ccnd2*. The mRNA expression analysis of *Ins1, Ins2* and *Gcg* from fasted 6-month-old

WT, hCGβ+ and cabergoline-treated WT (WTcab) and hCGβ+ (hCGβ+cab) pancreata was carried out by qRT-PCR. ANOVA, followed by Bonferroni's post hoc test, was conducted. Different letters indicate a value of at least $p< 0.05$. Data are presented as mean mean±SEM (n=4). (B) immunolocalization of PDX1 and NKX 6.1 in pancreas. Representative sections from 6-month-old WT, hCGβ+ and hCGβ+cab female mice were immunostained with PDX1 and NKX 6.1 specific antibodies. Scale bar 100 μm.

Table 1. Metabolic characterization of 6-month-old WT and hCGβ+ female mice

	WT	hCGβ+
Body weight (g)	24,7 ± 0,7 (7)	34,9 ± 2,0*** (7)
Daily food intake (g/mouse)	4,42±0,20 (7)	4,43±0,27 (7)
Abdominal white fat (g)	1,79±0,35 (7)	3,72±0,42** (7)
Bio hCG (IU/L)	1,79 ± 0,15 (4)	23,46 ± 8,66*** (4)
Glucose (mg/dl)	152±7 (5)	145±10 (7)
Insulin (ng/ml)	0,21±0,07 (5)	1,07±0,21*** (7)
HOMA-IR	1,78±0,65 (5)	8,78±2,12** (7)
QUICKI	0,37±0.02 (5)	0,29±0.01** (7)
Triglycerides (mg/dl)	147±14 (5)	634±61 *** (5)
Cholesterol (mg/dl)	130±14 (4)	177±18 (5)
HDL-C (mg/dl)	82±4 (4)	95±5 (5)
Cholesterol/HDL ratio	1,59±0,18 (4)	1,86±0,14 (5)
Triglycerides/HDL ratio	1,78±0,11 (4)	6,79±0,22*** (5)

Data are presented as mean±SEM, the number of animals used in each determination is indicated in brackets. Student´s t-test: * $p<0,05$; ** $p<0,01$; *** $p<0,001$.

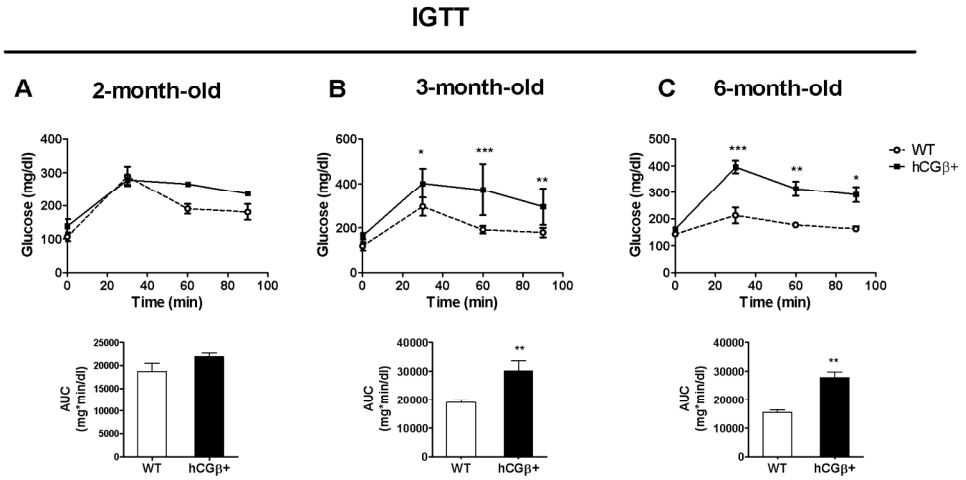

Figure 1. Intraperitoneal Glucose Tolerance Test (IGTT) in hCGβ+ female mice at 2, 3 and 6 month of age. IGTT (2 g/kg) in fasted WT and hCGβ+ females was performed at 2 (A), 3 (B) and 6 (C) months of age. Two-way ANOVA with repeated-measures, followed by Bonferroni's post hoc test was conducted; * p<0,05; ** p<0,01; *** p<0,001. The area under the curve (AUC) was analyzed for each group at different ages; Student´s t-test was conducted; ** p<0,01. Data are presented as mean±SEM (n=4-7).
165x86mm (300 x 300 DPI)

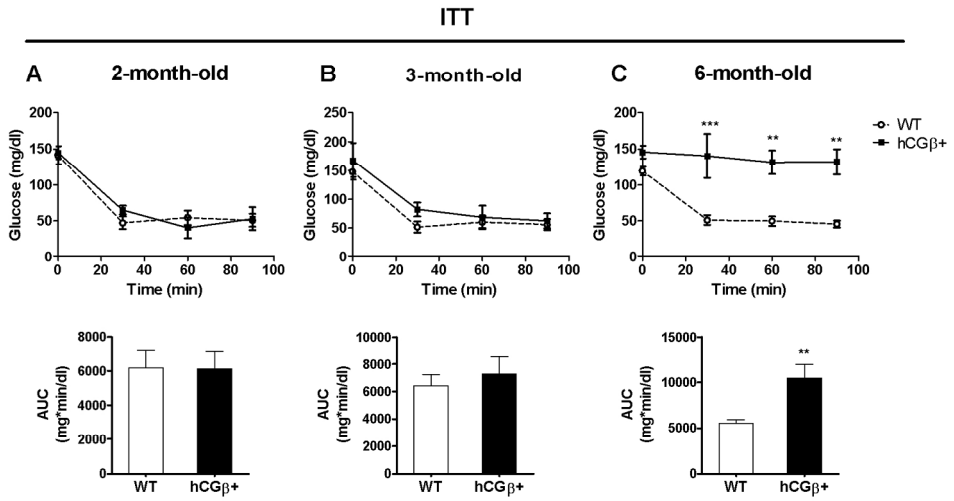

Figure 2. Intraperitoneal Insulin Tolerance Test (ITT) in hCGβ+ female mice at 2, 3 and 6 month of age. ITT (0,75 IU/kg) in fasted WT and hCGβ+ females was performed at 2 (A), 3 (B) and 6 (C) months of age. Two-way ANOVA with repeated-measures, followed by Bonferroni's post hoc test was conducted; * $p<0,05$; *** $p<0,001$. The area under the curve (AUC) was analyzed for each group at different ages; Student´s t-test was conducted; ** $p<0,01$. Data are presented as mean±SEM (n=4-7).
165x89mm (300 x 300 DPI)

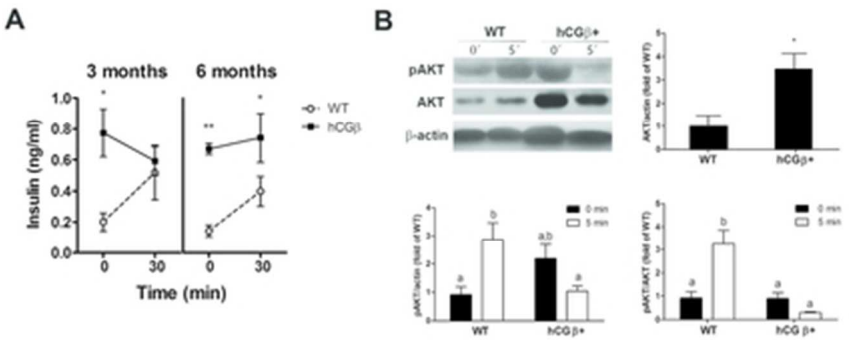

Figure 3. (A) Glucose- stimulated insulin release in 3- and 6-month-old hCGβ+ female mice. Glucose (2 g/kg) was administered i.p. to fasted WT and hCGβ+ female mice, and serum insulin levels were measured at 0 and 30 min post-glucose. Two-way ANOVA with repeated-measures, followed by Bonferroni's post hoc test was conducted. Data are presented as mean±SEM (n=4). *: P<0.05; **: p<0.01. (B) Peripheral tissue response to insulin. A representative western blot was shown for AKT activation in skeletal muscle. Samples were obtained from fasted 6-month-old WT and hCGβ+ female mice at 0 or 5 min after insulin administration. Two-way ANOVA followed by Bonferroni's post hoc test or Student's t-test was conducted according to each case. Different letters indicate a value of at least p<0.05. Data are presented as mean±SEM (n=4).
36x15mm (300 x 300 DPI)

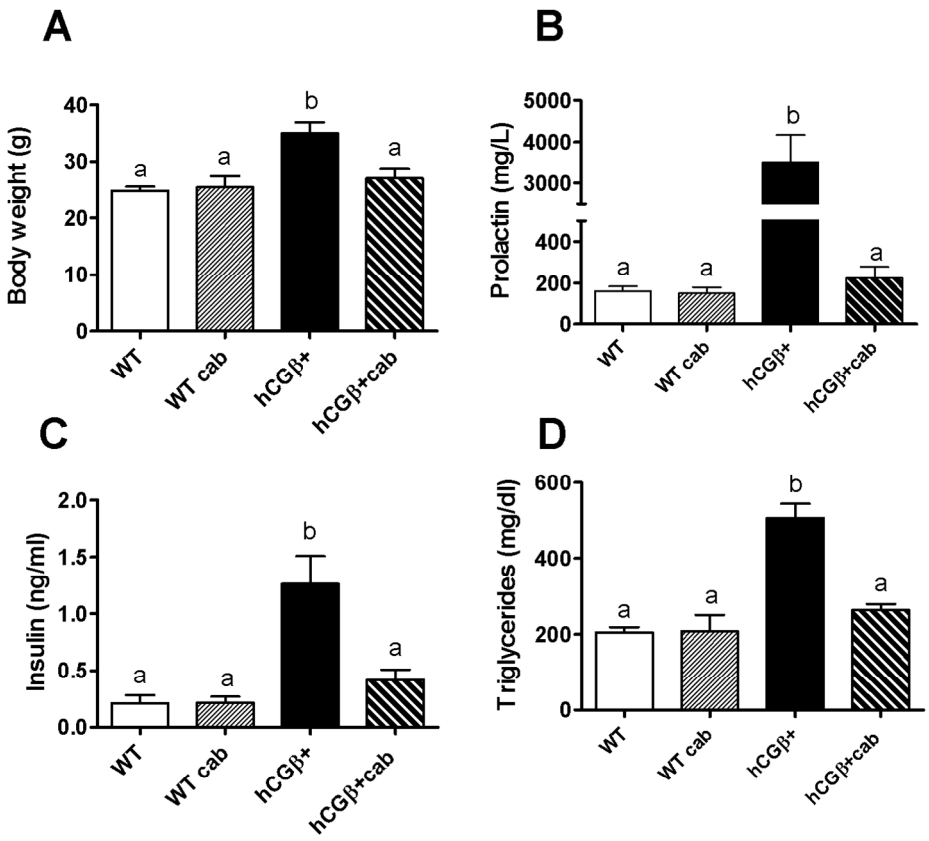

Figure 4. Effect cabergoline on body weight and serum levels of prolactin, insulin, and triglycerides in hCGβ+ females. Body weight (A) and serum prolactin (B), insulin (C) and trygicerides (D) levels in 6-month-old cabergoline- treated transgenic females (hCGβ+cab) after 18 hr fasting. WT, cabergoline-tretated WT (WTcab) and hCGβ+ females were used as controls. ANOVA, followed by Bonferroni's post hoc test was conducted. Different letters indicate a value of at least $p<0,05$. Data are presented as mean±SEM (n=4-12).
132x119mm (300 x 300 DPI)

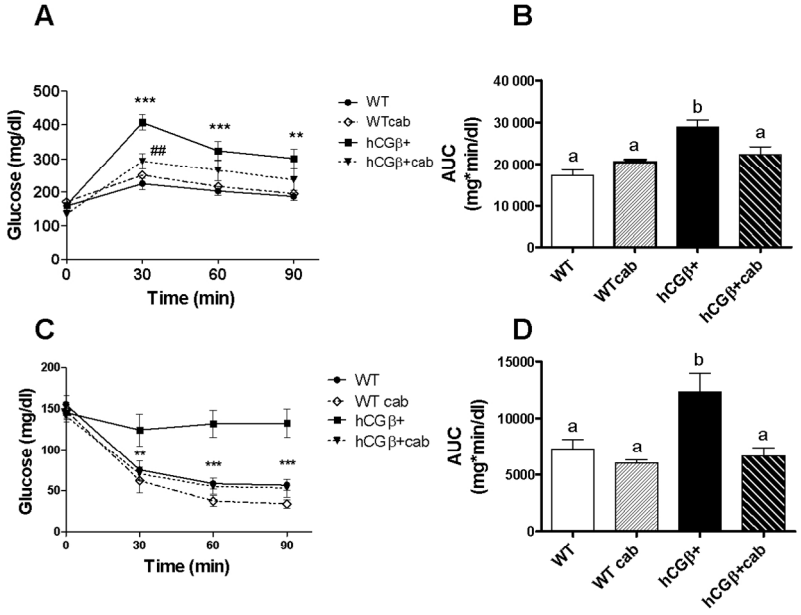

Figure 5. Effect of cabergoline treatment on the glucose homeostasis in WT and hCGβ+ females. IGTT (2 g/kg) (A), and ITT (0,75 IU/kg) (C) in fasted 6-month-old cabergoline- treated transgenic (hCGβ+cab) females was performed; fasted 6-month-old WT, cabergoline-treated WT (WTcab) and hCGβ+ females were used as control groups. Two-way ANOVA with repeated-measures, followed by Bonferroni's post hoc test was conducted. A) WT vs hCGβ+ **: p<0,01; ***: p<0,001; hCGβ+ vs hCGβ+cab ##: p<0,01; C) hCGβ+ vs WT, WTcab, hCGβ+cab; **: p<0,01, ***: p<0,001. The area under the curve (AUC) was analyzed for the different groups (B, D). ANOVA followed by Bonferroni's post hoc test was conducted. Different letters indicate a value of at least p<0,05. Data are presented as mean±SEM (n=4-12).
132x87mm (300 x 300 DPI)

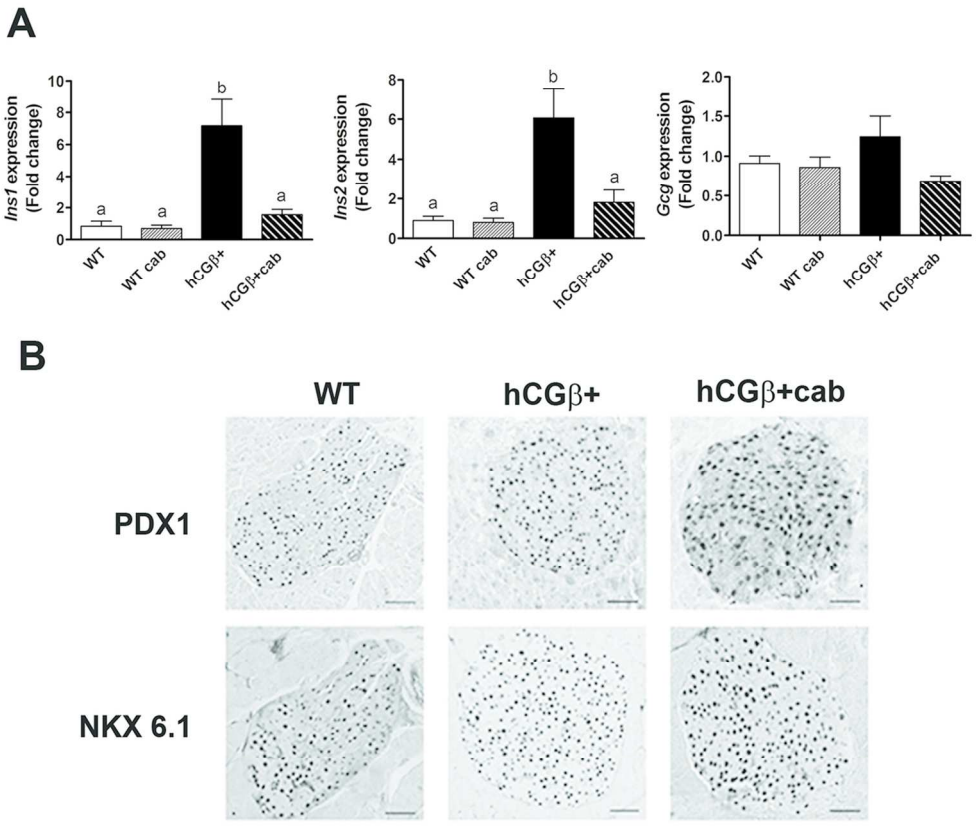

Figure 6. (A) Effect of cabergoline on the pancreatic gene expression of Ins1, Ins2, Gcg and Ccnd2. The mRNA expression analysis of Ins1, Ins2 and Gcg from fasted 6-month-old WT, hCGβ+ and cabergoline-treated WT (WTcab) and hCGβ+ (hCGβ+cab) pancreata was carried out by qRT-PCR. ANOVA, followed by Bonferroni's post hoc test, was conducted. Different letters indicate a value of at least $p < 0.05$. Data are presented as mean mean±SEM (n=4). (B) immunolocalization of PDX1 and NKX 6.1 in pancreas. Representative sections from 6-month-old WT, hCGβ+ and hCGβ+cab female mice were immunostained with PDX1 and NKX 6.1 specific antibodies. Scale bar 100 μm.
130x112mm (300 x 300 DPI)